Scripta Materialia 127 (2017) 1–5

Contents lists available at ScienceDirect

Scripta Materialia

journal homepage: www.elsevier.com/locate/scriptamat

Regular Article

Elastocaloric effect in a $Co_{50}Ni_{20}Ga_{30}$ single crystal

Ao Shen [a,b,c], Dewei Zhao [b,c], Wen Sun [b,c], Jian Liu [b,c,*], Caiju Li [a,**]

[a] Faculty of Materials Science and Engineering, Kunming University of Science and Technology, 650093 Kunming, China
[b] Key Laboratory of Magnetic Materials and Devices, Ningbo Institute of Material Technology and Engineering, CAS, Ningbo 315201, China
[c] Zhejiang Province Key Laboratory of Magnetic Materials and Application Technology, Ningbo Institute of Material Technology and Engineering, CAS, Ningbo 315201, China

ARTICLE INFO

Article history:
Received 21 June 2016
Received in revised form 23 August 2016
Accepted 24 August 2016
Available online 5 September 2016

Keywords:
Shape memory alloy
Martensitic transformation
Elastocaloric effect

ABSTRACT

Elastocaloric effect for a $Co_{50}Ni_{20}Ga_{30}$ single crystal has been investigated. A local adiabatic temperature change (ΔT) of −6 K was observed on the removal of a uniaxial stress of 150 MPa at 291 K. Infrared thermography measurement reveal a correlated response of martensitic bands and temperature mapping. Both elastocaloric effect and superelasticity exhibit a good reversibility in the 100 times of cycling test. The experimentally obtained ΔT value agrees well with the theoretical one by analyzing the temperature dependence of critical stress based on the Clausius-Clapeyron equation.

© 2016 Acta Materialia Inc. Published by Elsevier Ltd. All rights reserved.

Recently, elastocaloric effect (eCE) has been considered as a good candidate to substitute the traditional vapor compression refrigeration for its energy saving and environmental protection [1–4]. The eCE refers to the caloric effect induced by a uniaxial stress. Since the first result of a giant eCE in shape memory alloys (SMAs) was reported on a Cu-Zn-Al single crystal [5], the eCE has been widely investigated in SMAs [6–9]. In these alloys, eCE has been designed based on the uniaxial stress induced martensitic transformation (MT), which is accompanied by a large latent heat absorption and release. The eCE can be characterized by adiabatic temperature change (ΔT). Direct measurement of ΔT has been reported in Cu-Zn-Al, Ni-Ti, Ni-Fe-Ga-(Co) and Ni-Mn-based SMAs [6–9]. In traditional SMAs, a giant temperature rise of 25 K has been observed in a Ti-Ni wire on stretching [6], and the Cu-Zn-Al polycrystalline bulk has been reported to show a ΔT of 6–7 K over a large temperature span [7]. More recently, a large ΔT of 9–10 K has been demonstrated in the $Ni_{50}Fe_{19}Ga_{27}Co_4$ ferromagnetic SMA under a compressive stress of 300 MPa [10]. In Ni-Mn-based metamagnetic SMAs, a reversible ΔT of 3–4 K was reported [11,12]. It can be seen that the eCE has a number of advantages for solid-state refrigeration applications such as large and reversible ΔT, wide temperature window and low driving force.

The stress-induced MT has been widely reported in Co-Ni-Ga ferromagnetic SMAs [13–17]. In 2006, Dadda et al. reported that the [001] oriented $Co_{49}Ni_{21}Ga_{30}$ single crystal can exhibit superelastic behavior in a wide temperature range up to 385 K [13]. This wide temperature window originates from the low critical stress (σ_c) for the stress-induced MT and high yield strength of the sample. Besides, a low value of σ_c of 40 MPa and an excellent cyclic stability of superelastic behavior near room temperature have also been reported in the single crystal with the same composition [15]. The outstanding superelastic behavior and good mechanical properties indicate that Co-Ni-Ga alloys have the potential of good eCE. However, the eCE in Co-Ni-Ga system has not been studied so far. In this work, we report a large eCE in a $Co_{50}Ni_{20}Ga_{30}$ single crystal near room temperature, which is related to a first order transformation between a high-temperature austenitic phase exhibiting $L2_1$ structure with lattice parameters of a = 5.743 Å at 313 K and a lower-temperature martensitic phase exhibiting $L1_0$ structure with lattice parameters of a = b = 5.422 Å and c = 6.401 Å (c/a = 1.18) at 203 K [18]. The time-resolved temperature profiles of the sample during compression tests have been investigated by infrared (IR) thermography measurements.

The nominal composition $Co_{50}Ni_{20}Ga_{30}$ ingot was prepared by induction melting under an argon atmosphere and then used to grow single crystal by optical floating zone method in an inert nitrogen atmosphere. Rectangular samples in size of 4 mm × 4 mm × 8 mm with the long axis along the growth direction were cut from the as-grown crystal for compression tests. X-ray pole-density scans were carried out in a four-circle goniometer based on Schulz reflection geometry by X-ray diffraction with Co K_α radiation (λ = 0.179 nm) (BRUKERAXS D8 DISCOVER). Magnetization versus temperature curves were measured by superconductive quantum interference device (SQUID, Quantum Design MPMS-5S). Room-temperature compression and cyclic loading experiments were conducted on a universal testing machine (SUNS UNTM5000) with the measurement of strain by an extensometer and ΔT by a K-type thermocouple pasted on the middle of the sample surface. The high-temperature compression experiments in 296–393 K were conducted on another universal testing machine (WDW-20). In

* Correspondence to: Jian Liu, Key Laboratory of Magnetic Materials and Devices, Ningbo Institute of Material Technology and Engineering, CAS, Ningbo 315201, China.
** Corresponding author.
E-mail addresses: liujian@nimte.ac.cn (J. Liu), lcj@kmust.edu.cn (C. Li).

http://dx.doi.org/10.1016/j.scriptamat.2016.08.030
1359-6462/© 2016 Acta Materialia Inc. Published by Elsevier Ltd. All rights reserved.

order to display the local temperature evolution of the sample, an IR camera with a frame rate of 10 Hz was used to record the temperature-time profiles. When performing the ΔT measurement, a high strain rate of 2% s^{-1} was used to approach an adiabatic condition.

实验结果与讨论

Fig. 1(a) shows the magnetization as a function of temperature in a magnetic field of 100 Oe for the $Co_{50}Ni_{20}Ga_{30}$ single crystal. The sudden variations in magnetization correspond to the forward and reverse MTs. The MT starts at $M_s = 246.5$ K and finishes at $M_f = 230$ K on cooling, while the reverse MT starts at $A_s = 245.5$ K and finishes at $A_f = 264$ K on heating. The thermal hysteresis, indicating the nature of first order transition, is calculated to be 17.5 K. Fig. 1(b) shows the pole figure of the single crystal at room temperature. Four {220} poles can be observed and they are fourfold rotational symmetric. Such phenomenon indicates that the austenitic sample has a cubic structure with an excellent sole orientation. The four {220} poles do not distribute symmetrically about the center in Fig. 1(b). This implies that the long axis of the sample deviates from [100] direction of the single crystal. The deviated angle is calculated to be 10.5°.

Fig. 2(a) shows the stress-strain curves for the $Co_{50}Ni_{20}Ga_{30}$ single crystal with different strain levels at 291 K with a loading strain rate of 0.02% s^{-1} and an unloading strain rate of 2% s^{-1}. The stress plateaus in the loading and unloading curves represent the strain-driven MT and reverse MT, respectively. The σ_c for each MT is nearly 75 MPa. To characterize the eCE, temperature-time profiles were obtained simultaneously with the compression curves by thermocouple measurements. The corresponding temperature-time profiles at different strain levels during the unloading process are shown in Fig. 2(b). Large ΔT caused by the reverse MT is observed in all the temperature-time profiles and the absolute value of ΔT increases with the increasing strain. To clarify the relationship between the applied strain and ΔT, a series of ΔT corresponding to different strain levels was measured, as shown in Fig. 2(c). When the strain is smaller than 4.6%, the absolute value of ΔT shows an initial increase with the increase of strain, which is attributed to the increase of transformed volume fraction. When further increasing the strain larger than 4.6%, the MT completed and the value of ΔT maintains at the same level of about −4.4 K. Fig. 2(d) shows temperature dependence of critical stress (σ_c) for the $Co_{50}Ni_{20}Ga_{30}$ single crystal (σ_c can be estimated from Fig. S1. in the Supplementary material [23]). The σ_c linearly increases with temperature in the range of 296–393 K, which can be fitted by:

$$\sigma_c = 1.99 \times (T - 273) + 41.37 \quad (1)$$

where T is the ambient temperature during each compression test. The slope $\frac{d\sigma_c}{dT} = 1.99$ MPa/K is almost equal to the previously reported one for the $Co_{49}Ni_{21}Ga_{30}$ single crystal [13].

Fig. 3(a) shows the stress-strain curve with a strain rate of 2% s^{-1} for the $Co_{50}Ni_{20}Ga_{30}$ single crystal and a series of infrared thermography images recorded simultaneously upon loading and unloading process. In this test, the sample was loaded up to the strain of 4.6% to ensure a complete transition, and subsequently unloaded after holding the maximum strain for 20 s to reach a thermal equilibrium between the sample and the environment. Upon loading, the evolution of the local temperature bands with an angle of 42° with respect to the loading direction can be monitored. The appearance of the temperature bands represents the lattice distortion that can be described by a shear of the {110} planes along the $\langle 1\bar{1}0 \rangle$ direction [19]. With the strain increasing, the temperature bands broaden in width along with the MT and heat transfer. When the maximum strain reached, the temperature bands vanish and temperature distributes nearly uniformly. During mechanical unloading, the temperature bands firstly appear at the edges of sample, and then propagate towards the center of the sample with the strain decreasing. Such a propagation of temperature bands has been described by finite element simulation in reference [20]. The minima of temperature finally focus on the temperature band in the center of the sample. The final state of temperature distribution is obviously different from that in the loading process.

The time dependence of the average temperature obtained by the IR camera for the detected surface is shown in Fig. 3(b). It can be seen that a reversible ΔT of 3.7 K is obtained in the $Co_{50}Ni_{20}Ga_{30}$ single crystal. Temperature-time profiles for two points (point A and point B) in the detected surface are also shown in Fig. 3(b) to display the difference of temperature distribution between the loading and unloading processes. Points A and B show a highest temperature change upon loading and a lowest temperature change upon unloading, respectively. It should be noticed that the absolute values of maximum ΔT in the loading and unloading processes are not equal at both points. Point A shows a maximum ΔT of 4.6 K in the loading process and a minimum ΔT of −3.4 K in the unloading process. For point B, the maximum ΔT in the loading process is 4 K and the minimum ΔT is −6 K in the unloading process. Due to the fact that the sample and the indenter are separated during unloading process, the efficiency of heat transfer is lower in the unloading process than in the loading process. The ineffective heat transfer may lead to a spatially inhomogeneous distribution of temperature change in the unloading process. However, the distribution of temperature change in the loading process is spatially uniform due to the efficient heat transfer. As a result, the ΔT in the two processes is asymmetric. So, it is the non-adiabatic conditions that determine the difference in the temperature change between loading and unloading curves.

Fig. 4(a) shows the ΔT as a function of temperature when unloading the stress of 200 and 300 MPa in the temperature range of 296–343 K. The strain rate was set up to 0.04% s^{-1} in the loading process and 2% s^{-1} in the unloading process. When unloading a stress of 200 MPa, the ΔT maintains at the maximum value of −5 K in 296–303 K. As the

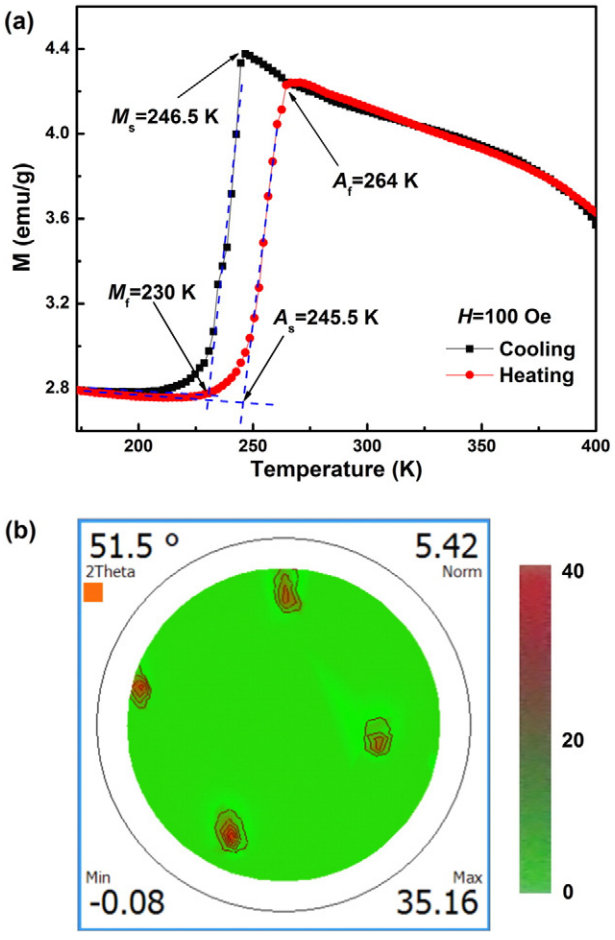

Fig. 1. (a) Temperature dependence of the magnetization in a magnetic field of 100 Oe for the $Co_{50}Ni_{20}Ga_{30}$ single crystal. (b) {220} pole figure for the $Co_{50}Ni_{20}Ga_{30}$ single crystal.

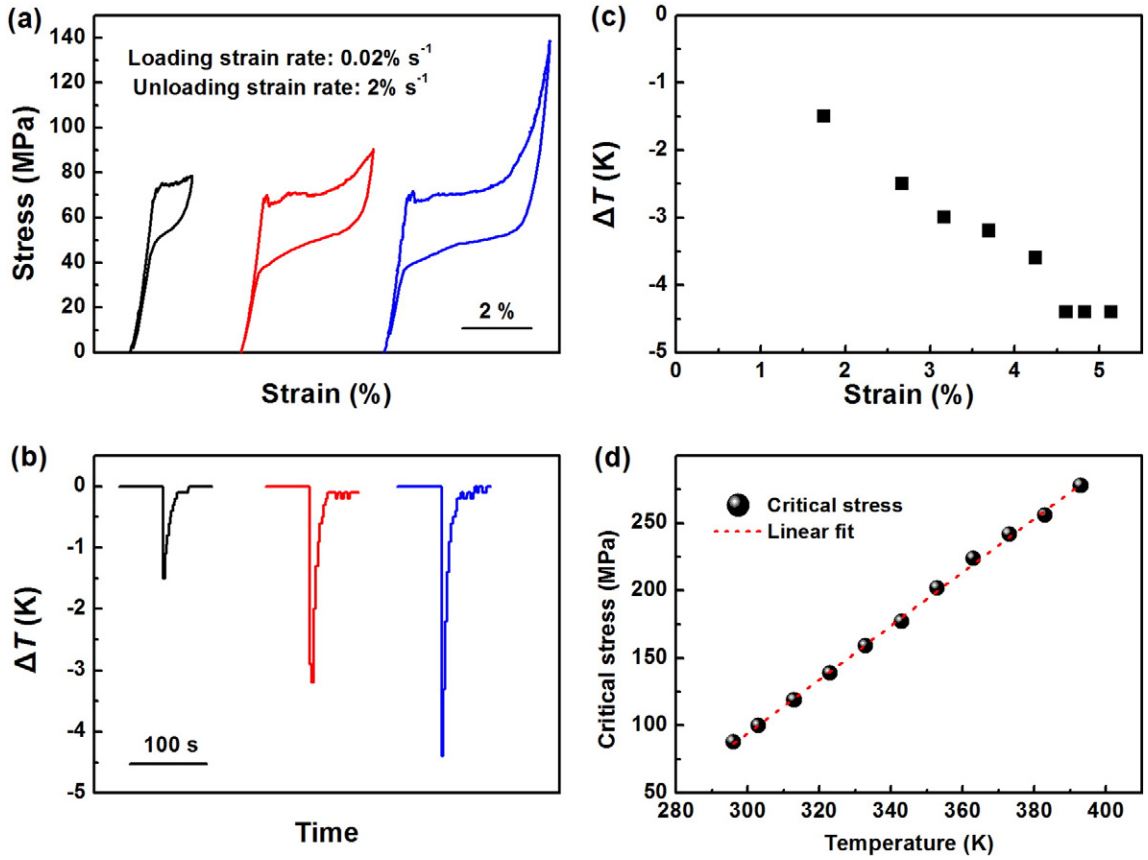

Fig. 2. (a) Stress-strain curves for the $Co_{50}Ni_{20}Ga_{30}$ single crystal with different strain levels at 291 K with a loading strain rate of 0.02% s^{-1} and an unloading strain rate of 2% s^{-1}. (b) Temperature-time profiles at different strain levels in the unloading process. (c) ΔT as a function of the applied strain. (d) Temperature dependence of σ_c for the $Co_{50}Ni_{20}Ga_{30}$ single crystal.

sample was heated to the temperature in the range of 303–343 K, the absolute value of ΔT decreases with increasing temperature. When the temperature was higher than 353 K, the temperature change is negligible. This may be estimated by Eq. (1) that when the temperature is higher than 352.7 K, the σ_c will be larger than 200 MPa. The applied stress of 200 MPa was not large enough to induce MT, so the removal of 200 MPa would not induce the inverse MT. In the absence of phase transformation, the ΔT would be too small to be detected. Nevertheless, there still can be observed a small magnitude of caloric effect in elastic region, e.g. $\Delta T = 0.1$ K at 383 K. While in the case of unloading a stress of 300 MPa, the maximum value of ΔT is still nearly −5 K in 296–343 K. However, the absolute value of ΔT gradually decreases from 5 K to 2.9 K as the temperature further increased from 343 K to 393 K. The ΔT calculated by Eq. (1) would not drop to zero until the sample is heated above 403 K.

To investigate the mechanical stability of $Co_{50}Ni_{20}Ga_{30}$ single crystal, a cycling test (up to 100 times) was conducted under a compressive stress of 200 MPa with the loading rate of 0.04% s^{-1} and unloading rate of 2% s^{-1}. Fig. 4(b) shows the selected stress-strain curves of the cycling test and Fig. 4(c) shows the temperature as a function of time at every 10th of the cycling test. As shown in Fig. 4(b), with increasing of cycle number, the stress plateau ascends slightly for the first 50 cycles and nearly maintains at the same level for the second 50 cycles. The magnitude of transformation strains does not show obvious change and the curves can completely recover during each unloading process, which indicates the good cyclic ability. The temperature change shown in Fig. 4(c) range from 4.8 K to 5.5 K with a small fluctuation, which indicates the high stability of the eCE in the cycling test.

Compared with the absolute value of maximum ΔT measured by thermocouple, the maximum ΔT of 6 K measured by the IR camera is much larger. This is because that the frequency for the thermocouple (1 Hz) is much lower than that for the IR camera (10 Hz) and the thermocouple only reflects the average temperature of the small area where it pasted. As can be seen from Fig. 3(a), the temperature in the surface of sample varies with time and location. Therefore, the maximum ΔT measured by thermocouple may be different even for the complete phase transformation.

The adiabatic temperature change associated with the elastocaloric effect can be approximately estimated as:

$$\Delta T \approx -\left(\frac{T}{C_p}\right) \times \Delta S \tag{2}$$

where C_p is the specific heat, T is the ambient temperature during compression tests and ΔS is the entropy change of the phase transformation. C_p is assumed to be stress independent and can be approximately considered to be 25 J/mol K for the $Co_{50}Ni_{20}Ga_{30}$ single crystal in both martensitic and austenitic phases [21]. ΔS can be calculated from Clausius-Clapeyron equation:

$$\Delta S = -\varepsilon_t \times \frac{d\sigma_c}{dT} \times \frac{1}{\rho} \tag{3}$$

where $\frac{d\sigma_c}{dT}$ is the critical stress dependence on temperature, ρ is the mass density and ε_t is the transformation strain. For the $Co_{50}Ni_{20}Ga_{30}$ single crystal, values of $\frac{d\sigma_c}{dT}$, ρ and ε_t are taken as 1.99 MPa/K, 8.55×10^3 kg/m^3 and 3.7% (the 3.7% is taken from the Fig. S2. in supplementary material [23]), respectively. The calculated ΔS for the $Co_{50}Ni_{20}Ga_{30}$ single crystal is about 8.6 J/kg K. Thus, the value of ΔT calculated from Eq. (2) is 6.2 K. From this, one can see that the calculated ΔT value almost equals to the directly measured one, which further confirms the fact that the MT is completed when the applied strain is 4.6% within error and the strain

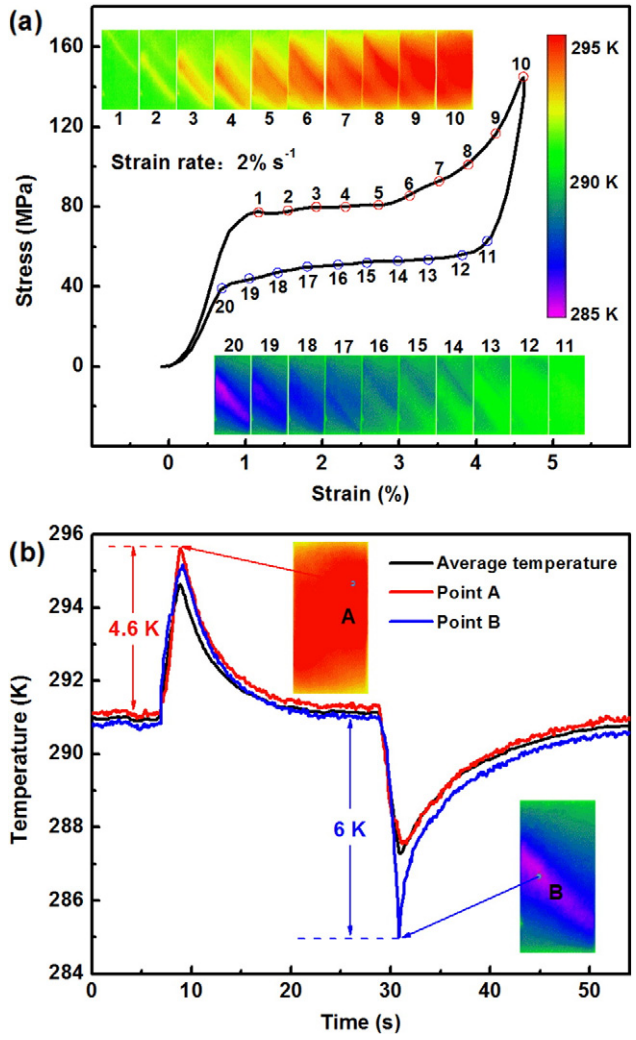

Fig. 3. (a) Stress-strain curve for the $Co_{50}Ni_{20}Ga_{30}$ single crystal at 291 K with a strain rate of 2% s^{-1} and a series of infrared thermography images recorded simultaneously with the compress curves. Images are numbered consecutively. The time interval between two adjacent images is 0.2 s. (b) Temperature-time profile of the point A point B as well as the average temperature of detected surface.

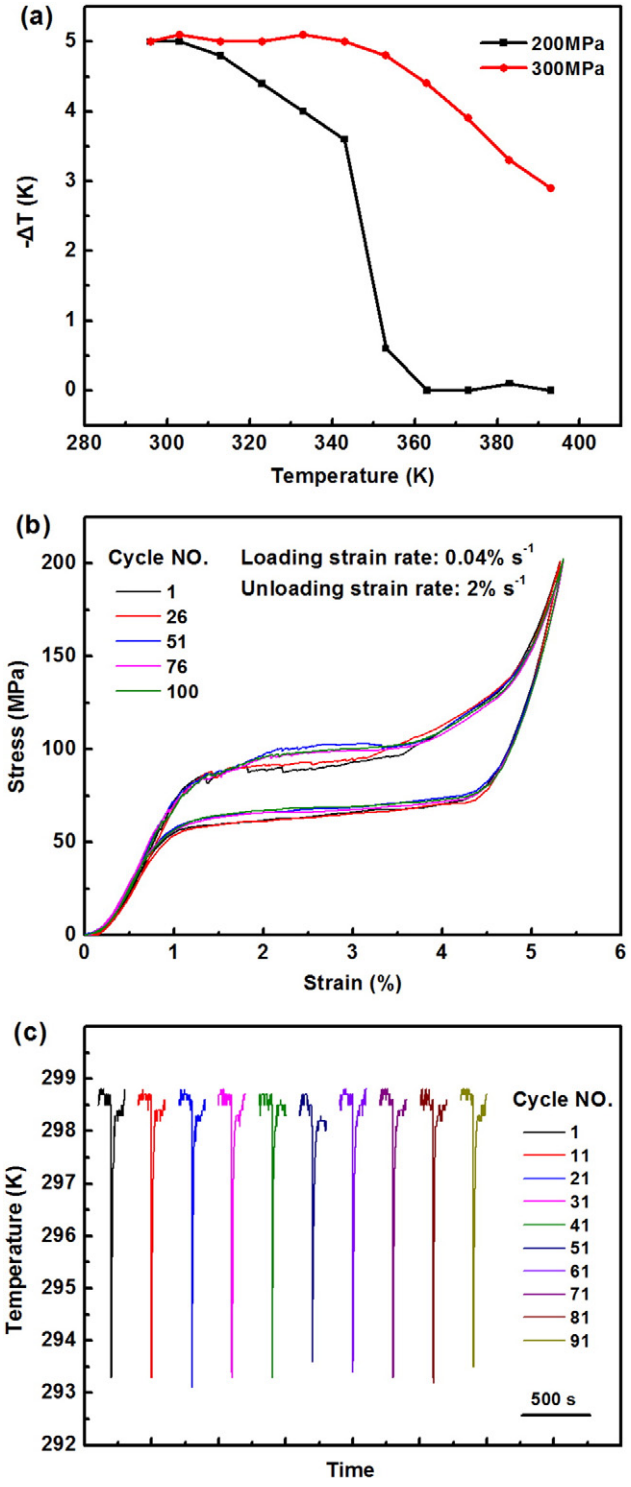

Fig. 4. (a) ΔT as a function of temperature when unloading the stress of 200 and 300 MPa in the temperature range of 296–343 K. (b) Stress-strain curve of cyclic loading experiments. (c) Temperature as a function of time at every 10th of the cycling test.

rate of 2% s^{-1} is high enough to approach an adiabatic condition in the unloading process (while in the case of loading process, the indenter compresses the sample tightly and the approximation of adiabatic condition is worse). The absolute value of ΔT for a complete MT in the $Co_{50}Ni_{20}Ga_{30}$ single crystal is lower than those calculated in other eCE systems (15.5 K in $Ni_{45}Mn_{44}Sn_{11}$ alloy [22], 10 K in $Ni_{54}Fe_{19}Ga_{27}$ single crystal [8] and 12.6 K in Ni-Mn-In-Co alloy [11]). According to the Eqs. (2) and (3), the affecting factors of both ΔS and ΔT are ε_t and $\frac{d\sigma_c}{dT}$, where the value of 3.7% for ε_t is moderate when compared with other alloy systems. It is important to point out that the value of $\frac{d\sigma_c}{dT}$ for Co-Ni-Ga is relatively smaller compared with those observed in other eCE systems (8.75 MPa/K in Ni-Ti foil [20], 4.2 MPa/K in Ni-Mn-In alloy [9] and 3.3 MPa/K in $Ni_{54}Fe_{19}Ga_{27}$ single crystal [8]). Therefore, a further improved eCE in the Co-Ni-Ga system strongly relies on the increase of $\frac{d\sigma_c}{dT}$.

结论

In summary, we have investigated the elastocaloric effect in a $Co_{50}Ni_{20}Ga_{30}$ single crystal. A full martensitic transformation can be achieved with the strain of 4.6%. The value of ΔT is found to be related to the transformed volume fraction and a maximum temperature change of −6 K have been detected for a completed reverse MT by IR camera. Besides, IR thermography measurement reveals a correlated response of martensitic bands and temperature mapping and the evolution of temperature change can be greatly influenced by heat transfer. The completed MTs are maintained in the temperature range of 296–343 K by application the stress of 300 MPa and the sample shows good reversibility and cyclability during 100 times of cycling test. The theoretical calculation of ΔT for a complete MT indicates that the relatively low ΔT in the $Co_{50}Ni_{20}Ga_{30}$ single crystal is due to the low dependence of critical stress on temperature. For further

investigation, more efforts should be put into increasing the critical stress dependence on temperature.

The research leading to these results has received funding from the National Natural Science Foundation of China (grant nos. 51371184, 51531008 and 51361017).

Appendix A. Supplementary data

Supplementary data to this article can be found online at http://dx.doi.org/10.1016/j.scriptamat.2016.08.030.

References

[1] X. Moya, S. Kar-Narayan, N.D. Mathur, Nat. Mater. 13 (2014) 439–450.
[2] M. Schmidt, A. Schütze, S. Seelecke, Int. J. Refrig. 54 (2015) 88–97.
[3] S. Crossley, N.D. Mathur, X. Moya, AIP Adv. 5 (2015) 067153.
[4] L. Mañosa, A. Planes, M. Acet, J. Mater. Chem. A 1 (2013) 4925–4936.
[5] E. Bonnot, R. Romero, L. Mañosa, E. Vives, A. Planes, Phys. Rev. Lett. 100 (2008) 125901.
[6] J. Cui, Y.M. Wu, J. Muehlbauer, Y. Hwang, R. Radermacher, S. Fachler, M. Wuttig, I. Takeuchi, Appl. Phys. Lett. 101 (2012) 073904.
[7] L. Mañosa, S. Jarque-Farnos, E. Vives, A. Planes, Appl. Phys. Lett. 103 (2013) 211904.
[8] Y. Xu, B.F. Lu, W. Sun, A.R. Yan, J. Liu, Appl. Phys. Lett. 106 (2015) 201903.
[9] Y.J. Huang, Q.D. Hu, N.M. Bruno, J.H. Chen, I. Karaman, J.H. Ross Jr., J.G. Li, Scr. Mater. 105 (2015) 42–45.
[10] F. Xiao, M.J. Jin, J. Liu, X.J. Jin, Acta Mater. 96 (2015) 292–300.
[11] B.F. Lu, F. Xiao, A.R. Yan, J. Liu, Appl. Phys. Lett. 105 (2014) 161905.
[12] B.F. Lu, P.N. Zhang, Y. Xu, W. Sun, J. Liu, Mater. Lett. 148 (2015) 110–113.
[13] J. Dadda, H.J. Maier, I. Karaman, H.E. Karaca, Y.I. Chumlyakov, Scr. Mater. 55 (2006) 663–666.
[14] I.V. Kuksgauzen, I.V. Kireeval, Y.I. Chumlyakov, H. Maier, IOP Conf. Series: Materials Science and Engineering 93, 2015 012033.
[15] J. Dadda, H.J. Maier, D. Niklasch, I. Karaman, H.E. Karaca, Y.I. Chumlyakov, Metall. Mater. Trans. A 39 (2008) 2026–2039.
[16] V.A. Chernenko, J. Pons, E. Cesari, A.E. Perekos, Mater. Sci. Eng. A 378 (2004) 357–360.
[17] P. Krooß, P.M. Kadletz, C. Somsen, M.J. Gutmann, Y.I. Chumlyakov, W.W. Schmahl, H.J. Maier, T. Niendorf, Shap. Mem. Superelasticity 2 (2016) 37–49.
[18] F.B. Meng, Y.X. Li, H.Y. Liu, J.P. Qu, M. Zhang, G.Q. Liu, Z.H. Liu, X.F. Dai, J.L. Chen, G.H. Wu, Mater. Sci. Forum 475 (2005) 2033–2036.
[19] A. Planes, L. Mañosa, Solid State Phys. 55 (2001) 159–267.
[20] H. Ossmer, F. Lambrecht, M. Gültig, C. Chluba, E. Quandt, M. Kohl, Acta Mater. 81 (2014) 9–20.
[21] D.L. Schlagel, T.A. Lograsso, A.O. Pecharsky, Mater. Res. Soc. Symp. Proc. 785 (2004) 219.
[22] W. Sun, J. Liu, B.F. Lu, Y. Li, A.R. Yan, Scr. Mater. 114 (2016) 1–4.
[23] See Supplementary material at http://dx.doi.org/10.1016/j.scriptamat.2016.08.030. Fig. S1. shows the stress-displacement curve for $Co_{50}Ni_{20}Ga_{30}$ single crystal at different temperatures. The displacement refers to the displacement of crossbeam, which includes the deformation of both sample and the long indenter. The arise of transformation could be observed by the change of slope on stress-displacement curves. Since the stress is accurate, the critical stresses could be obtained from Fig. S1. Fig. S2. shows the stress-strain for the $Co_{50}Ni_{20}Ga_{30}$ single crystal when the sample was loaded and unloaded at a slow strain rate of 0.01% s^{-1} near room temperature (T = 291 K). The strain rate was set up to 0.01% s^{-1} to ensure an isothermal condition during the loading-unloading process since the Clausius-Clapeyron calculations should be used in isothermal process. As can been seen from Fig. S2., the ε_t could be estimated to be 3.7%.